



This is a repository copy of *Substructuring of dynamical systems via the adaptive minimal control synthesis algorithm*.

White Rose Research Online URL for this paper:  
<http://eprints.whiterose.ac.uk/79675/>

Version: Accepted Version

---

**Article:**

Wagg, D.J. and Stoten, D.P. (2001) Substructuring of dynamical systems via the adaptive minimal control synthesis algorithm. *Earthquake Engineering and Structural Dynamics*, 30 (6). 865 - 877. ISSN 0098-8847

<https://doi.org/10.1002/eqe.44>

---

**Reuse**

Unless indicated otherwise, fulltext items are protected by copyright with all rights reserved. The copyright exception in section 29 of the Copyright, Designs and Patents Act 1988 allows the making of a single copy solely for the purpose of non-commercial research or private study within the limits of fair dealing. The publisher or other rights-holder may allow further reproduction and re-use of this version - refer to the White Rose Research Online record for this item. Where records identify the publisher as the copyright holder, users can verify any specific terms of use on the publisher's website.

**Takedown**

If you consider content in White Rose Research Online to be in breach of UK law, please notify us by emailing [eprints@whiterose.ac.uk](mailto:eprints@whiterose.ac.uk) including the URL of the record and the reason for the withdrawal request.



[eprints@whiterose.ac.uk](mailto:eprints@whiterose.ac.uk)  
<https://eprints.whiterose.ac.uk/>

# SUBSTRUCTURING OF DYNAMICAL SYSTEMS VIA THE ADAPTIVE MINIMAL CONTROL SYNTHESIS ALGORITHM

D. J. WAGG\* AND D. P. STOTEN<sup>†</sup>

*Faculty of Engineering, University of Bristol, Queens Building, University Walk, Bristol BS8 1TR, U.K.*

## SUMMARY

In this paper we consider the concept of modelling dynamical systems using numerical-experimental substructuring. This type of modelling is applicable to large or complex systems, where some part of the system is difficult to model numerically. The substructured model is formed via the adaptive minimal control synthesis (MCS) algorithm. The aim of this paper is to demonstrate that substructuring can be carried out in real time, using the MCS algorithm. Thus we reformulate the MCS algorithm into a substructuring form. We introduce the concepts of a transfer system, and carry out numerical simulations of the substructuring process using a coupled three mass example. These simulations are compared with direct simulations of a three mass system. In addition we consider the stability of the substructuring algorithm, which we discuss in detail for a class of second order transfer systems. A numerical-experimental system is considered, using a small scale experimental system, for which the substructuring algorithm is implemented in real time. Finally we discuss these results, with particular reference to the future application of this method to modelling large scale structures subject to earthquake excitation.

KEY WORDS: adaptive control; numerical-experimental substructuring; real time control; modelling large structures; earthquake excitation

---

Draft version. February 14, 2000

\*Research assistant. Departments of Civil and Mechanical Engineering. [David.Wagg@bristol.ac.uk](mailto:David.Wagg@bristol.ac.uk), TEL: +44 117 9546832, FAX: +44 117 9287783

<sup>†</sup>Professor of Dynamics and Control, Department of Mechanical Engineering, [d.p.stoten@bristol.ac.uk](mailto:d.p.stoten@bristol.ac.uk), TEL: +44 117 9288208

## INTRODUCTION

The size and complexity of many dynamical systems makes accurate predictive modelling of dynamic behaviour difficult. This is particularly true for large scale engineering structures such as bridges and dams, where design engineers often use experimental model testing of the structure, in addition to theoretical and numerical modelling. Large scale testing facilities such as shaking tables and reaction walls have been used for many years to carry out experimental modelling for such structures<sup>?</sup>. However, because of size and weight limitations full scale dynamic testing is impossible for most large structures. As a result, often complex experimental test results have to be interpreted with the additional problem of scaling between the model and the full size structure.

For numerically simulating modular structures or those with a high degree of self similarity the technique of *substructuring*<sup>?</sup> has been developed to reduce the computational workload. The concept of subdividing a structure can also be used to formulate a model where one (or more) of the substructures is a physical test specimen. In this case the model of the overall structure is a combination of a numerical and an experimental model.

This type of combined modelling is particularly suitable to structures where a design critical element can be identified. Critical elements are those which are most difficult to model numerically, or most likely to fail during dynamic loading, and as such are of primary interest to the design engineer — in other words, parts of the structure which exhibit nonlinear or unpredictable behaviour. In this case the critical element would be modelled using a physical test specimen while the remainder of the structure is modelled numerically. The advantage of this method over scale model testing is that the critical element is tested at full size and the problems associated with scaling are eliminated.

The numerical–experimental substructuring technique has been used for testing large scale structures<sup>?</sup> using a *pseudodynamic* approach<sup>?</sup> in which dilated time scales are used, so that loading is applied to the structure quasi-statically. These tests are often performed using reaction wall facilities, where the reaction forces induced in the structure can be measured accurately, but real time inertia forces have to be estimated numerically. The concept of pseudodynamic testing has been extended to real time scales for single degree of freedom systems without substructuring<sup>?</sup> by using a dynamic actuator, for the purpose of testing velocity dependent components.

A more direct way of simulating the effects of dynamic loading on a structure is to use a shaking table. In this case forces on the structure are induced dynamically, in real time, a situation that

*EARTHQUAKE ENGINEERING AND STRUCTURAL DYNAMICS (2001) Vol. 30 pp865–877*  
cannot be realised by the pseudodynamic approach. By extending the concept of numerical–experimental substructuring to real time testing, the use of shaking table facilities can give more realistic modelling of the dynamic response of complex structures to dynamic loading?. This is the overall aim of this current research.

To produce such a combined numerical–experimental model some part of the two systems must be synchronised using a control algorithm. Here we use the minimal control synthesis (MCS) adaptive control algorithm?. This algorithm is classed as a model reference adaptive controller, which can be used without the need for system identification of the controlled system’s parameters.

In this current work we demonstrate how the MCS algorithm can be reformulated to form a substructure model for a dynamical system containing nonlinear (or other unknown) elements. In addition, using the passivity concept, we describe the stability proof for the substructured algorithm. We also present numerical simulations of a three mass system example to demonstrate the viability of this form of substructuring as a modelling technique. Finally we present implementation results using an experimental system as part of a substructuring model.

## THEORETICAL FORMULATION

The aim of the substructuring process is to model the dynamical behaviour of the overall system using a part numerical, part experimental model. Thus we refer to the overall system we wish to model as the structure and the physical test specimen as the substructure. The remaining part of the overall system is modelled numerically, and we refer to this as the numerical model. The combined numerical-experimental model is referred to as the substructured model.

The dynamics of the structure are governed by a general system of equations

$$\dot{w}(t) = h(w, t) \tag{1}$$

where  $w$  is the state vector of the overall system,  $h(\cdot)$  denotes an arbitrary function, and an overdot represents differentiation with respect to time  $t$ . Effectively, the aim of the substructuring process is to model the dynamics of  $h(\cdot)$ . Typically, we wish to characterise the dynamic response of the overall system subject to some excitation signal  $r(t)$ , such as an earthquake.

In general, the form of  $h(\cdot)$  is not known explicitly, but we assume that it can be split into linear and nonlinear parts, so that

$$\dot{w}(t) = Hw(t) + Gr(t) + \hat{h}(w, t) \tag{2}$$

where  $r(t)$  is the excitation signal,  $G$  is a gain matrix,  $H$  is a matrix representing the linear part of  $h$ , and  $\hat{h}$  the nonlinear (i.e. the difficult to model) part. To formulate a substructured model we separate the overall system dynamics, equation 2, so that the linear dynamics are modelled numerically, and the nonlinear dynamics are modelled using a physical test specimen.

To separate the two parts of the model, we divide the coordinates  $w$  into a subset associated with the nonlinear part,  $x_c \subset w$ , and those which represent the numerical model,  $z = \{z \in \mathbb{R}^{2m} : z \notin x_c\}$ . Thus  $x_c$  represents the state of the critical element(s) of the system. For the numerical model, we assume that the system is second order, so the  $m$  represents the degree of freedom of the numerical system. Now equation 2 can be expressed as

$$\begin{bmatrix} \dot{z} \\ \dot{x}_c \end{bmatrix} = \begin{bmatrix} H_1 & H_2 \\ H_3 & H_4 \end{bmatrix} \begin{bmatrix} z \\ x_c \end{bmatrix} + \begin{bmatrix} G_1 \\ G_2 \end{bmatrix} r + \begin{bmatrix} \hat{h}_1(z, x_c, t) \\ \hat{h}_2(z, x_c, t) \end{bmatrix} \quad (3)$$

The dynamics of the numerical model are linear, so  $\hat{h}_1(z, x_c, t) = 0$ . The dynamics represented by  $H_2x_c$  map to a series of experimental measurements  $H_2x_c \mapsto Rf(t)$ ,  $f(t) \in \mathbb{R}^q$ ,  $R \in \mathbb{R}^{2m \times q}$ , where  $f(t)$  is a vector of experimental measurements, and  $R$  is a transformation matrix. Typically experimental measurements would consist of forces, displacements or accelerations. Note that nonlinear dynamics could be included in the numerical model if known. Here we define “known” as linear, and “unknown” as nonlinear for simplicity. We also assume that  $G_2$  is a null matrix, such that the excitation is restricted to the numerical model. In addition, we restrict the size of the excitation vector  $r \leq m$ , to be at most equal to the degree of freedom of the numerical model.

The numerical model can now be extracted from equation 3 to give

$$\dot{z}(t) = H_1z(t) + G_1r(t) + Rf(t) \quad (4)$$

The values of  $f(t)$  recorded from the experiment are included in this expression via the conversion matrix  $R$  in place of the  $H_2x_c$  term.

In a similar manner, an equation for the dynamics of  $x_c$  could be extracted from equation 3. However, as we are assuming that the nonlinearity defined by  $\hat{h}_2$  is unknown, this is unnecessary. Using the experimental measurements  $f(t)$ , equation 4 becomes the substructured model of the system.

## THE CONTROL SYSTEM

The numerical model and the substructure are coupled linearly by the matrix  $H$ . To simulate this coupling between the two parts of the model, a *transfer system* is required which allows the numerical and experimental parts to interact. This would typically be an experimental testing facility such as a shaking table.

To perform a substructuring test, the substructure is mounted on the transfer system. Then equation 4 is evaluated using a suitable numerical method, in discrete time steps, subject to the excitation  $r(t)$ . At the same time, the transfer system is driven by a control signal to track the output from the numerical model, and  $f(t)$  is fed back into the numerical model. This process is carried out in *real time* so that appropriate inertia forces can be induced on the substructure. As a result, accurate control of the transfer system is essential to perform realistic substructuring tests.

In general we consider the dynamics of the transfer system to be linear and of the form

$$\dot{x}(t) = Ax(t) + Bu(t) + f(t) \quad (5)$$

where  $x \in \mathbb{R}^{2n}$  is the state vector of the transfer system,  $A \in \mathbb{R}^{2n \times 2n}$  and  $B \in \mathbb{R}^{2n \times p}$  are constant matrices and  $u(t) \in \mathbb{R}^p$  is the control signal. Thus  $\{A, B\}$  represents the dynamic parameters of the transfer system.

Here we are assuming that  $f(t)$  is the vector of forces imposed on the transfer system by the substructure, such that  $q = 2n$ . The force vector  $f(t)$  effectively acts as a disturbance on the transfer system, and due to the coupling between the numerical model and substructure, it is possible for  $f(t)$  to vary significantly during a test. Therefore the use of an adaptive controller is preferable, as the effect of the disturbance on the transfer system cannot be known in advance.

#### *The minimal control synthesis approach*

The adaptive scheme adopted in this current work is the minimal control synthesis (MCS) algorithm which has been developed at Bristol<sup>7, 8</sup>. This algorithm is particularly suited to substructuring for two reasons. Firstly, it is a model reference control algorithm, and the standard reference model can be conveniently substituted for the numerical model of the substructured system. Secondly, the algorithm requires no system identification, so that it can operate without explicit values for the matrices  $A$  and  $B$  of the transfer system. This also applies to the dynamics

of the substructure and the numerical model, which are not required to be known for effective controller implementation.

The control signal for the MCS algorithm is defined as

$$u(t) = K(t)x(t) + K_r(t)r(t) \quad (6)$$

where  $r(t) \in \mathbb{R}^p$  is the reference signal,  $K(t)$  is the feedback adaptive gain and  $K_r(t)$  the feed forward adaptive gain. The task of the controller is to drive the transfer system to replicate the motion of the output from the numerical model. We denote the output of the numerical model to be  $x_m \in \mathbb{R}^{2n}$ , where  $x_m \subset z$ ,  $m \geq n$ . The error signal between the required output from the numerical model and the motion of the transfer system is  $x_e = x_m - x$ . This error signal indicates the success of the control process, and as a result the overall accuracy of the method. The overall aim of the control algorithm is that  $x_e \rightarrow 0$  as  $t \rightarrow \infty$ . A schematic diagram of the complete substructuring system using MCS control is shown in Figure 1.

If  $z$  is divided into two sub-vectors such that  $z = [z_m, x_m]^T$ , where  $\dim(x_m) = 2n \times 1$  and  $\dim(z_m) = (2m - 2n) \times 1$ . Then equation 4 can be written in the form

$$\begin{bmatrix} \dot{z}_m \\ \dot{x}_m \end{bmatrix} = \begin{bmatrix} H_{11} & H_{12} \\ H_{13} & H_{14} \end{bmatrix} \begin{bmatrix} z_m \\ x_m \end{bmatrix} + \begin{bmatrix} G_{11} \\ G_{12} \end{bmatrix} r + \begin{bmatrix} R_1 \\ R_2 \end{bmatrix} f \quad (7)$$

Now  $\dot{x}_m$  represents the ‘‘reference model’’ dynamics, and  $\dot{z}_m$  represents the remaining numerical model dynamics. Extracting the reference model dynamics from equation 7 gives

$$\dot{x}_m(t) = H_{13}z_m(t) + H_{14}x_m(t) + G_{12}r(t) + R_2f(t) \quad (8)$$

where  $H_{13}$  is an  $2n \times (2m - 2n)$  matrix,  $H_{14}$  is  $2n \times 2n$ ,  $G_{12}$  is a  $2n \times p$  matrix and  $R_2$  is a  $2n \times 2n$  matrix. To standardise the notation with the conventional MCS formulation let  $A_m = H_{14}$ ,  $B_m = G_{12}$ ,  $H_m = H_{13}$  and  $R_m = R_2$ . Then equation 8 can be expressed as

$$\dot{x}_m(t) = A_mx_m(t) + B_mr(t) + H_mz_m(t) + R_mf(t) \quad (9)$$

which is similar to the standard MCS reference model form with the addition of the  $H_mz_m(t)$  and  $R_mf(t)$  terms. If we subtract equation 5 from equation 9, substituting for  $u(t)$  from equation 6, the error dynamics of the system are given by

$$\dot{x}_e = A_mx_e + (A_m - A - BK)x + (B_m - BK_r)r + d \quad (10)$$

where  $d(t) = H_mz_m + (R_m - I)f(t)$  is considered to be a disturbance. In fact, this disturbance comes from the coupled nature of the dynamics in the numerical model and the force feedback

*EARTHQUAKE ENGINEERING AND STRUCTURAL DYNAMICS (2001) Vol. 30 pp865–877*  
 from the substructure. Therefore this is an internal rather than an external disturbance for the substructured system. Other than this, equation 10 is now in a standard form for MCS error dynamics subject to a disturbance.

We also note that if  $R_m = I_{2n}$ , which it does in this case where we have assumed that  $f(t)$  is exactly the vector of forces experienced by the transfer system, then  $d(t) = H_m z_m$ . So, in this case the disturbance comes entirely from coupling within the numerical model. Furthermore, as the dynamics of the numerical model are linear, we can see that if the system is stable, the disturbance  $d(t)$  is always bounded.

### *Stability via passivity*

The stability of the error dynamics given in equation 10 can be proven using the concept of passivity<sup>?</sup>. For completeness we outline the main elements of the proof here.

The error dynamics of the system can be divided into forward and feedback adaptive dynamic blocks. This is illustrated schematically in Figure 2. In the figure, the system is driven by the disturbance signal  $d(t)$ , and the feedback dynamics are represented by  $\Phi^T w$ , where  $\Phi = [B^{-1}(A_m - A - BK) \quad | \quad B^{-1}(B_m - BK_r)]$  and  $w = [x^T, r^T]^T$ . The forward dynamics of the error system are given by

$$\dot{x}_e = A_m x_e + B_e B_c u_e, \quad y_e = C_e x_e, \quad u_e = \Phi^T w + d', \quad (11)$$

where  $C_e$  is a linear compensation matrix which ensures that the triple  $\{A_m, B_e, C_e\}$  is strictly positive real,  $B_e = [O_n, I_n]^T$ ,  $B_c$  is an  $n \times n$  matrix and  $d' = B^{-1}d$ . For a class of transfer systems  $g_e(s)$  between  $u_e$  and  $y_e$  such that  $y_e = g_e(s)B_c u_e$ , where  $B_c$  is positive definite symmetric, the forward dynamics can be shown to be dissipative<sup>?</sup>. Then by proving that the dynamics of the adaptive block are passive via the Popov criteria

$$\int y_e(-\Phi^T w) \geq -\gamma^2 \quad (12)$$

where  $\gamma$  is a finite constant, the complete system can be shown to be asymptotically stable<sup>?</sup>. Additional detailed information on the stability and robustness of the MCS algorithm is given in<sup>?</sup>.



The transfer systems we will consider take the form of a second order mechanical oscillator, represented by a generalised coordinate  $q \in \mathbb{R}^n$ , in the form

$$M_t \ddot{q} + D_t \dot{q} + K_t q = K_a u \quad (13)$$

where,  $M_t$ ,  $D_t$  and  $K_t$  are the mass, damping and stiffness matrices of the transfer system, and  $K_a$  is the actuator gain. For this system, the mass matrix,  $M$ , is positive definite by definition. In addition we will assume that by design,  $K_a$  can be taken as positive definite, and that all the parameter matrices are symmetric. For a transfer system in this Lagrangian form, equation 11 has coefficient matrices

$$A = \begin{bmatrix} 0_n & I_n \\ -M_t^{-1}K_t & -M_t^{-1}D_t \end{bmatrix}, \quad B = \begin{bmatrix} 0 \\ M_t^{-1}K_a \end{bmatrix} \quad (14)$$

in Lagrangian coordinate form. The matrix  $B$  can be written as  $B = B_e B_c$ , where  $B_e = [O_n, I_n]^T$  and  $B_c = M^{-1}K_a$  is a positive definite symmetric matrix. The plant matrix for the reference model,  $A_m$ , is of a similar structure to the  $A$  matrix, and is chosen to be stable, such that all the eigenvalues of  $A_m$  have negative real parts. For a substructuring system,  $A_m$  is a subset of the numerical model, so this condition places a restriction on the class of numerical models which can be used. If required  $K_a$  can be included as part of the feedback dynamics<sup>?</sup>.

The transfer function  $g_e(s)$  between  $y_e(s)$  and  $u_e(s)$  is  $C_e(sI - A_m)^{-1}B_e$ , such that  $y_e = g_e(s)B_c u_e$ . For this class of transfer systems,  $C_e$  can be chosen so that  $g_e(s)$  is strictly positive real, and hence the forward dynamics of equation 13 are dissipative.

## NUMERICAL EXAMPLE

We now consider a numerical example of a three mass oscillator system, which is shown schematically in Figure 3. This system is one of the simplest configurations which can be used to demonstrate the substructuring concept. The three masses are coupled by two linear springs  $k_1$  and  $k_2$ , and a nonlinear spring  $k_3$ . Each mass is independently damped by a viscous damper  $c_i$ ,  $i = 1, 2, 3$ . The system is forced via a support motion  $r(t)$ . Here we will compare the output from a direct simulation of the system with the output of a substructured model of the system, to demonstrate the viability of substructuring as a modelling technique. The equation of motion for the system

can be written as

$$M\ddot{\xi} + D\dot{\xi} + g(\xi) = Sr(t) \quad (15)$$

where,  $M$  and  $D$  are the mass, and damping matrices respectively, the stiffness is represented by  $g(\xi)$  and  $Sr(t)$ , represents the support excitation. Equation 15 represents the structure we wish to model, and can be expressed in first order form (as equation 1), where  $\hat{h}_1(w, t) = 0$ , and  $\hat{h}_2(w, t)$  represents the stiffness function,  $g(\xi)$ . In this example we will use a cubic spring nonlinearity in addition to a linear stiffness term to form  $g(\xi)$ .

To model this overall system we split it into a numerical model and substructure, which is shown, schematically, in Figure 4. Here, we have chosen mass  $m_3$  as the substructure, since  $k_3$  is the nonlinear part of the structure. This is mounted on the transfer system, mass  $m_t$ , which has stiffness  $k_t$  and damping  $c_t$ . The masses  $m_1$  and  $m_2$  correspond to the numerical model. The effect of  $m_3$  on  $m_1$  and  $m_2$  is now represented by the single measurement  $f(t)$  which in this case is a force. Note that selecting  $m_1$  or  $m_2$  as the substructure is more difficult. This would involve having *two* transfer systems, which experimentally would be more difficult to implement. We envisage that this type of system will form the subject of future work, especially with regard to the multiple support excitation of structures?

Writing the numerical model dynamics in the form of equation 4, gives

$$\dot{z} = \begin{bmatrix} 0_m & I_m \\ -M^{-1}K_s & -M^{-1}D \end{bmatrix} z + \begin{bmatrix} 0_m \\ M^{-1}S \end{bmatrix} r(t) + \begin{bmatrix} 0_m \\ I \end{bmatrix} f(t) \quad (16)$$

where we have used the Lagrangian formulation such that  $z \in \mathbb{R}^4 = [z_1, z_2, \dot{z}_1, \dot{z}_2]^T$ . Also

$$M = \begin{bmatrix} m_1 & 0 \\ 0 & m_2 \end{bmatrix}, K_s = \begin{bmatrix} k_1 + k_2 & -k_2 \\ -k_2 & k_2 \end{bmatrix}, D = \begin{bmatrix} c_1 & 0 \\ 0 & c_2 \end{bmatrix}, S = \begin{bmatrix} k_1 & 0 \\ 0 & 0 \end{bmatrix} \quad (17)$$

For this example, we see that by synchronising the motion of  $m_2$  and  $m_t$  using the control algorithm, the motion of  $m_1$ ,  $m_2$  and  $m_3$  should be the same for both the complete system, Figure 3, and the substructured model, Figure 4. The force  $f(t) = k_3((z_3 - x) + (z_3 - x)^3) + c_3\dot{z}_3$  can be computed (rather than measured) at each iteration, and it includes the effect of the nonlinear spring.

To compare the output of the two systems, we monitor the displacement of mass  $m_2$  and the transfer system mass,  $m_t$ . The displacement  $x$  of the mass  $m_t$  of the substructured system forced using a sine wave  $r(t) = 0.5 \times \cos(t)$  is shown in Figure 5 (a) as a solid line. The dashed line in

Figure 5 (a) shows the displacement of mass  $m_2$  of the overall system, Figure 3, using the same forcing.

It is worth emphasising that the output from the substructured model is not connected with the direct simulation of the three mass system in any way. So, in Figure 5 (a) we are plotting the output from two completely separate numerical systems. There is a good level correlation between the two signals, indicating that in this case the substructured model is a close representation of the overall system. We do not attempt to quantify the level of correlation between the two systems here. However, we note that the nonlinear nature of the systems means that during transient motion the dynamics are sensitive to small perturbations. As a result the dynamics of the substructured model may diverge from the overall system dynamics during transient motion, although steady state dynamics should converge (assuming that the initial conditions of both systems are suitably far from any basin of attraction boundaries). This aspect of the modelling procedure requires future investigation. The MCS adaptive gains are shown in Figure 5 (b). The gain signals are composed of several oscillatory components. This is typical of adaptive gains controlling a nonlinear system.

## NUMERICAL–EXPERIMENTAL EXAMPLE

Having demonstrated the substructuring concept using a purely numerical simulation, we now consider a true numerical–experimental system. Again we use the example of the three mass system shown in Figure 3. In this case we formulate a substructure model of the three mass system using a numerical two mass model and a *physical* two mass system. A photograph of the experimental setup for the physical two mass system is shown in Figure 6.

The masses are mounted on a uniaxial track with wheel bearings. Springs between the two end stops and the masses themselves provide the restoring forces for the central position of the masses. In this system the nonlinearity occurs due to friction in the bearings on which the masses oscillate. In this configuration one of the masses of the physical apparatus is used as the transfer system. The position of this mass ( $m_t$ ) is represented by the scalar coordinate,  $x$  and can be controlled via an electric motor. The second mass is chosen as the substructure (i.e equivalent to  $m_3$ ), and is allowed to vibrate freely. The displacement of the substructure is represented by the scalar coordinate  $x_c$ . The displacements,  $x$  and  $x_c$  and velocities  $\dot{x}$  and  $\dot{x}_c$  of the masses are measured using LVDT transducers and tachometers respectively. These signals were read via a

Amplicon PC30AT card, which was also used to output the control signal. A second order MCS controller was used which had gain wind-up protection<sup>2</sup>. This was implemented on a 486 Personal Computer running RedHat Linux 5.1 The substructuring algorithm ran at a sampling rate of 512Hz, using the Linux real-time clock.

The numerical part of the model used for this system, was similar to the example in previous example. Two masses were coupled by springs and damped independently, with displacement coordinates  $z_1$  and  $z_2$ . Parameters used were those of the physical system for the masses, 0.515 kg each, and spring stiffness which was measured as 2.43 N/m. Viscous damping was assumed for the model, and a value of 2.4 Ns/m was estimated to be approximately equivalent to the frictional damping in the physical system, for the range of forcing frequency used during testing. The reference output from the numerical model was taken as  $z_2$ , such that  $x_m = z_2$ .

The system was forced using a low frequency sine wave,  $0.1 \cos(0.1t)$ , to remain within the limits of the computer/acquisition hardware. The results of a typical test are shown in Figure 7. In Figure 7 the amplitude of displacement of the transfer system,  $x$ , is plotted along with the output from the numerical model,  $x_m$  and the displacement of the free mass,  $x_c$ . We see that for this set of parameter values, the controlled motion has some nonsmooth characteristics due to the frictional nature of the system. Despite this, in general the tracking is good. The effect of the free mass on the transfer system can be seen on the upward side of the response peaks, where the response of the transfer system is pulled away from the reference output.

The experimental two mass rig was fitted with three relatively light springs between the masses, which each had a stiffness of approximately 2.43 N/m. As a result the force feedback between the transfer system and substructure was quite low. This can be seen in the feedback force signal, which for this test is shown in Figure 8. The MCS gains for this test are shown in Figure 9. Again we note the periodic oscillation which occurs in the gains for a nonlinear system.

It is interesting to note that in this example, the transfer system was subject to the same nonlinearity as the substructure. However, the MCS controller was still effective in tracking the required signal.

## CONCLUSIONS

In this paper, we have discussed the concept of numerical-experimental substructuring. For a system which can be divided into linear (known) and nonlinear (unknown) parts, we have shown

how a substructured model can be formulated. A key aspect of such a system is the control system. We have used the minimal control synthesis (MCS) algorithm, which, because of its adaptive form, is particularly suited to substructuring. We have shown how the algorithm can be reformulated for substructuring, by substituting the standard reference model with the numerical model. When the transfer system is in the form of a second order mechanical oscillator, we have shown via the passivity theorem, that the system is asymptotically stable.

Using numerical simulations, we have demonstrated the concept of using a substructured model of a three mass system. The results from this system were compared to a direct simulation of the overall system, and a good level of agreement was observed. This demonstrates the viability of substructuring as modelling technique. However we have noted that the correlation between the output of the two numerical simulations is not unity due to the presence of nonlinearities. Future work is required to determine the accuracy of the substructured model, perhaps based on the error signal from the control algorithm. We have also shown results from a true numerical-experimental substructured system, which demonstrates the practical application of the substructuring algorithm.

In terms of modelling large scale structures, this work represents an initial step toward developing useful testing methods. We envisage future work will involve extending these results to large scale testing facilities, such as shaking tables. In such a testing environment it should be possible to use real time numerical-experimental substructuring to provide useful modelling results for large scale engineering structures.

#### ACKNOWLEDGEMENTS

This work was funded by DG12 of the European Commission as part of the HCMP-TMR-RTD research program in earthquake engineering, specifically grant No. ERBFMGECT-980103. In addition the authors would like to thank Eduardo Gómez Gómez for his assistance with the experimental work carried out for this paper.

FIGURE CAPTIONS

- Figure 1: Schematic representation of numerical experimental substructuring system with MCS control.
- Figure 2: Schematic representation of error dynamics as a feedback system.
- Figure 3: Schematic representation of a three mass system.
- Figure 4: Schematic representation of the substructured system used to model the three mass system in Figure 3.
- Figure 5: Three degree of freedom system, parameter values  $m_i = 1.0$  and  $c_i = 0.1$  for  $i = 1, 2, 3$ ,  $m_t = 1.0$ ,  $k_t = 1$  and  $c_t = 1.0$ . The stiffness  $k_1 = k_2 = 1.0$ , and  $k_3 = -\delta + \delta^3$  where  $\delta$  is the extension of the spring. A settling time of 0.01 was required and the step size used in the Runge-Kutta algorithm was 0.001. (a) Displacement of  $z_2$  of three mass system (dashed line) plotted against  $x$  from the substructured system (solid line). (b) Adaptive gains from the MCS algorithm,  $K_1$  solid line,  $K_2$  long dashes and  $K_r$  short dashes.
- Figure 6: Experimental two mass system.
- Figure 7: Displacement time series from two mass substructuring test showing output from the numerical model,  $x_m$ , displacement of the transfer system,  $x$ , and displacement of the free mass  $x_c$ . Sample rate 512Hz.
- Figure 8: Feedback force from two mass substructuring test. Sample rate 512Hz.
- Figure 9: MCS gains recorded during the two mass substructuring test. Sample rate 512Hz.

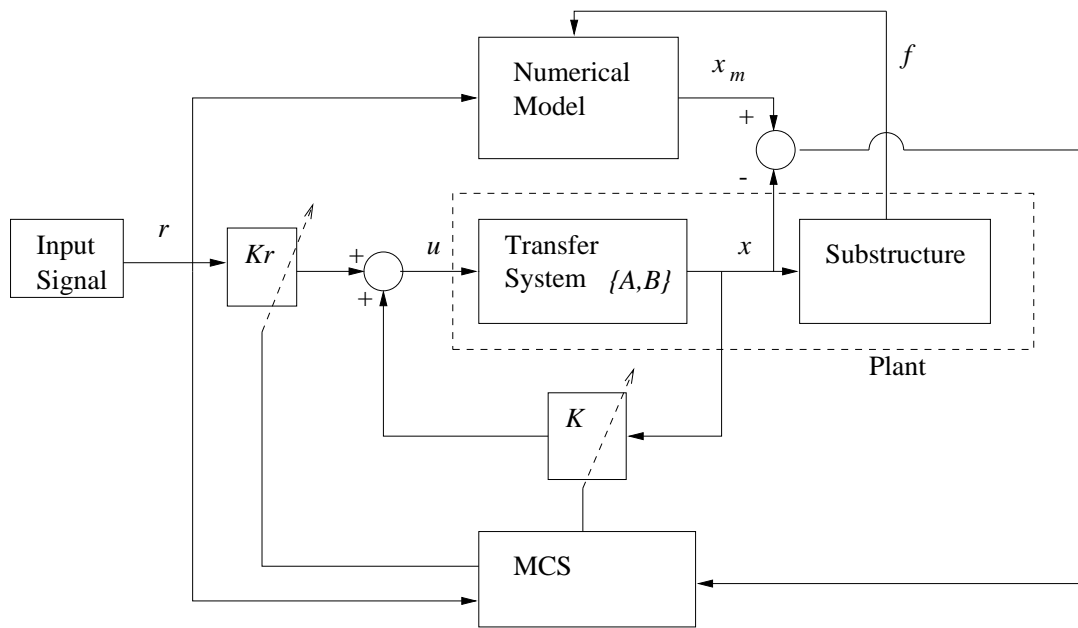


Figure 1:

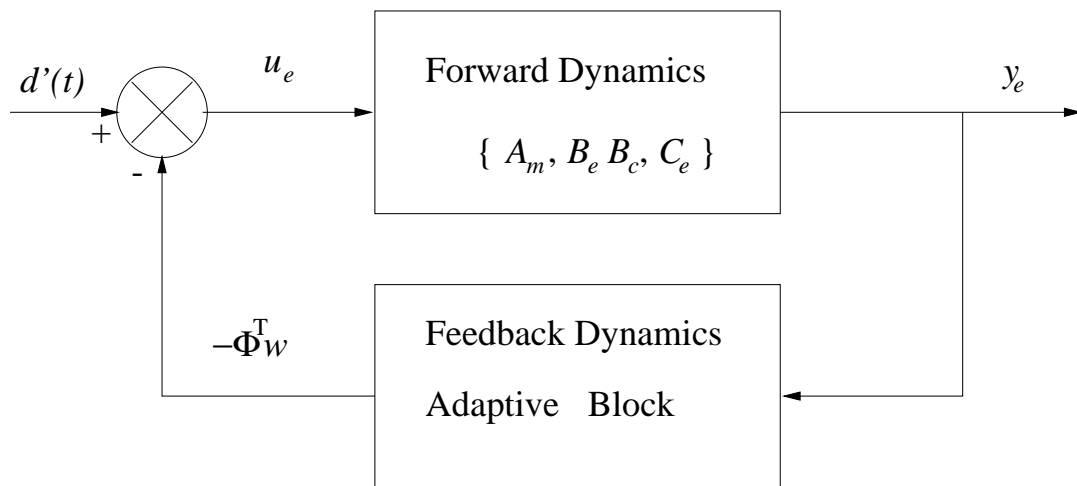


Figure 2:



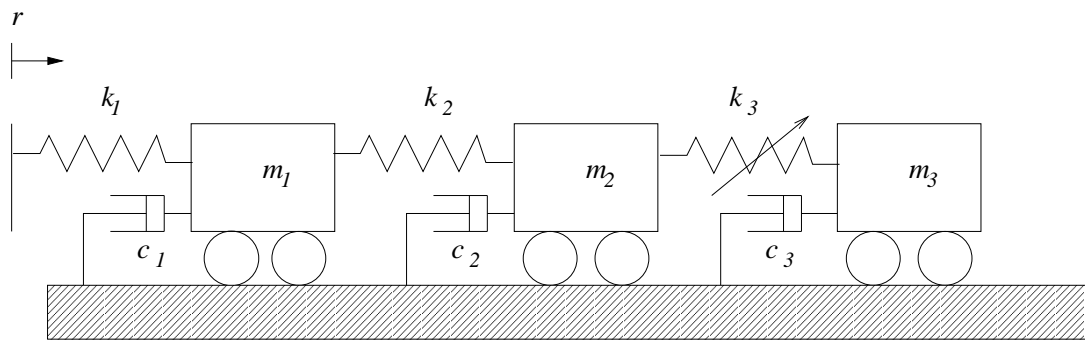


Figure 3:

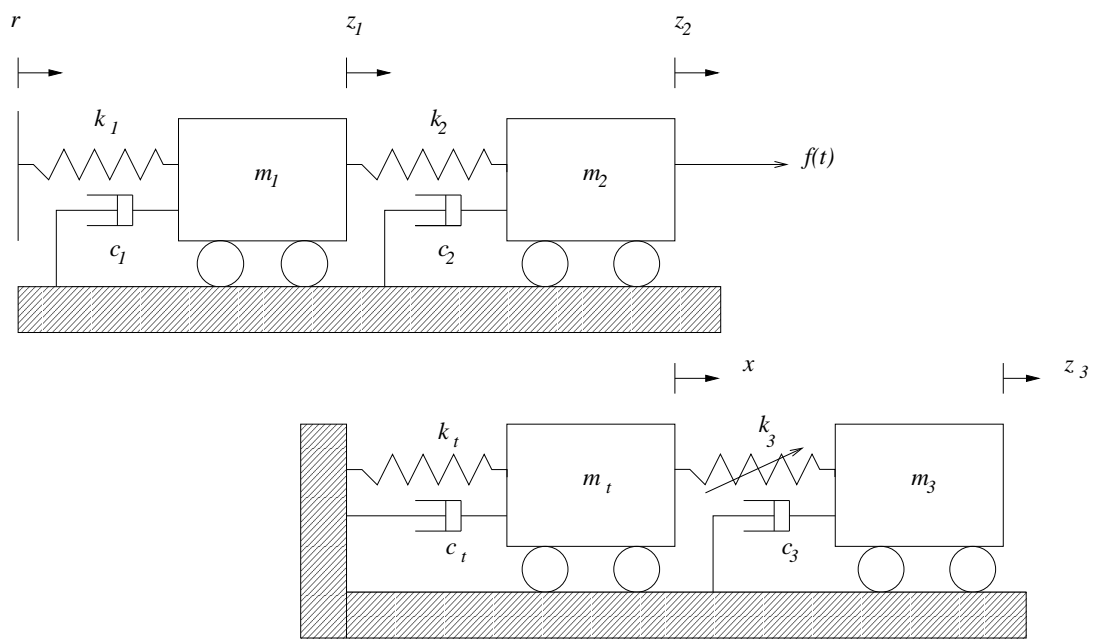
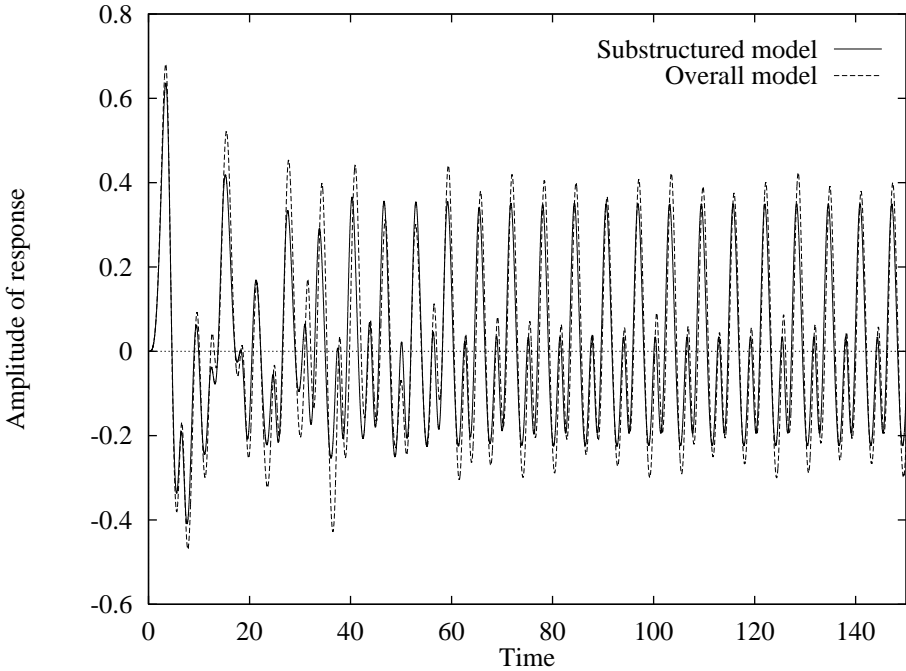
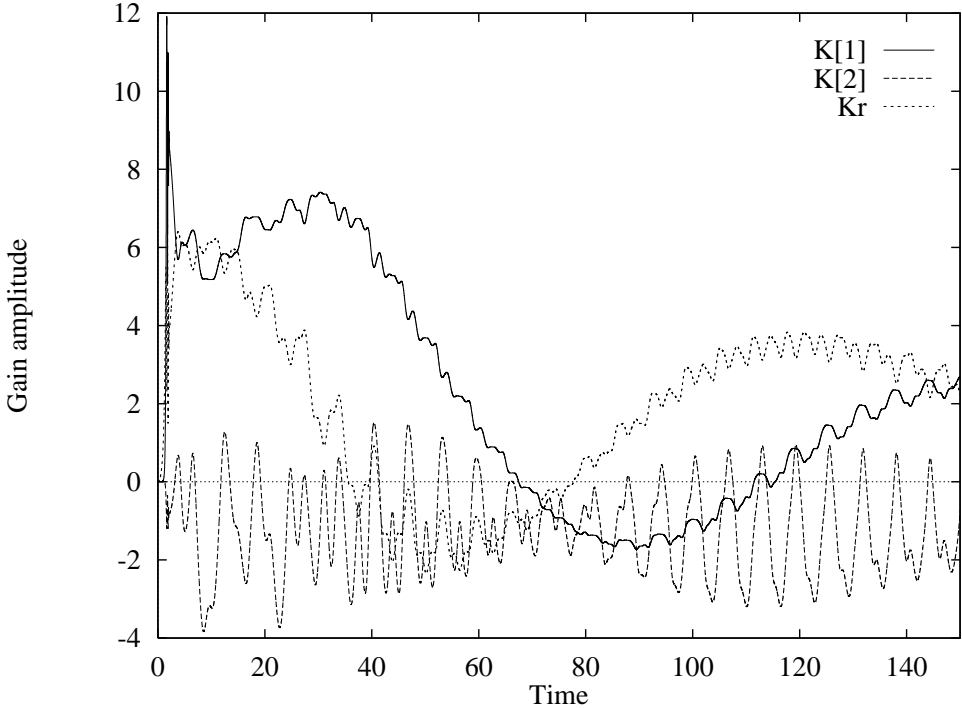


Figure 4:



(a)



(b)

Figure 5:



Figure 6:

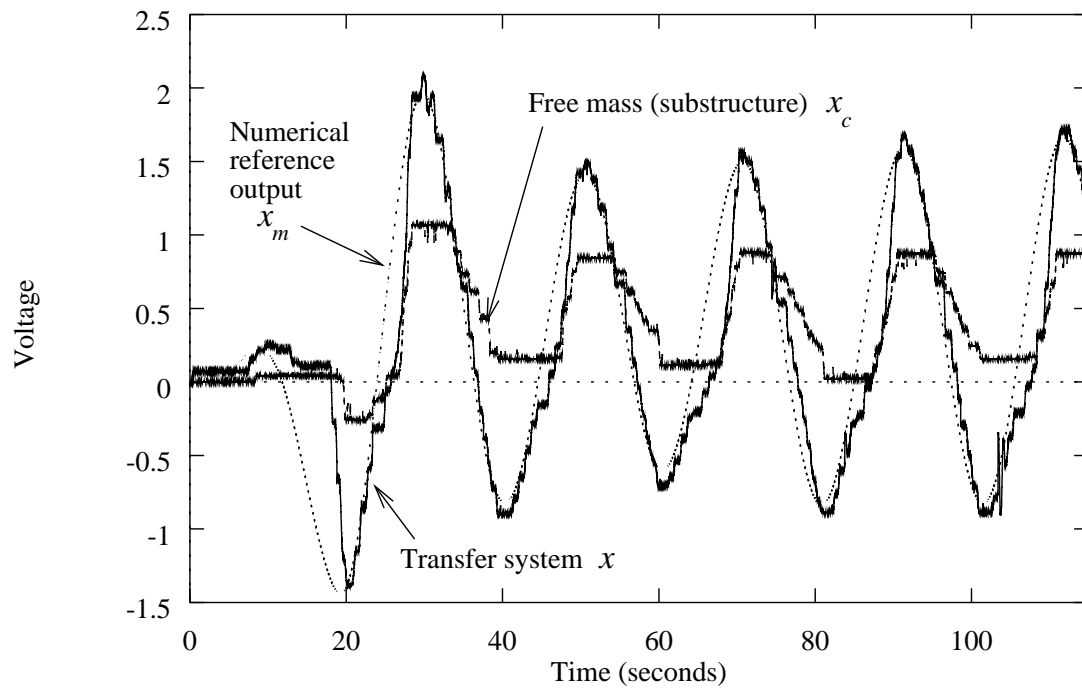


Figure 7:

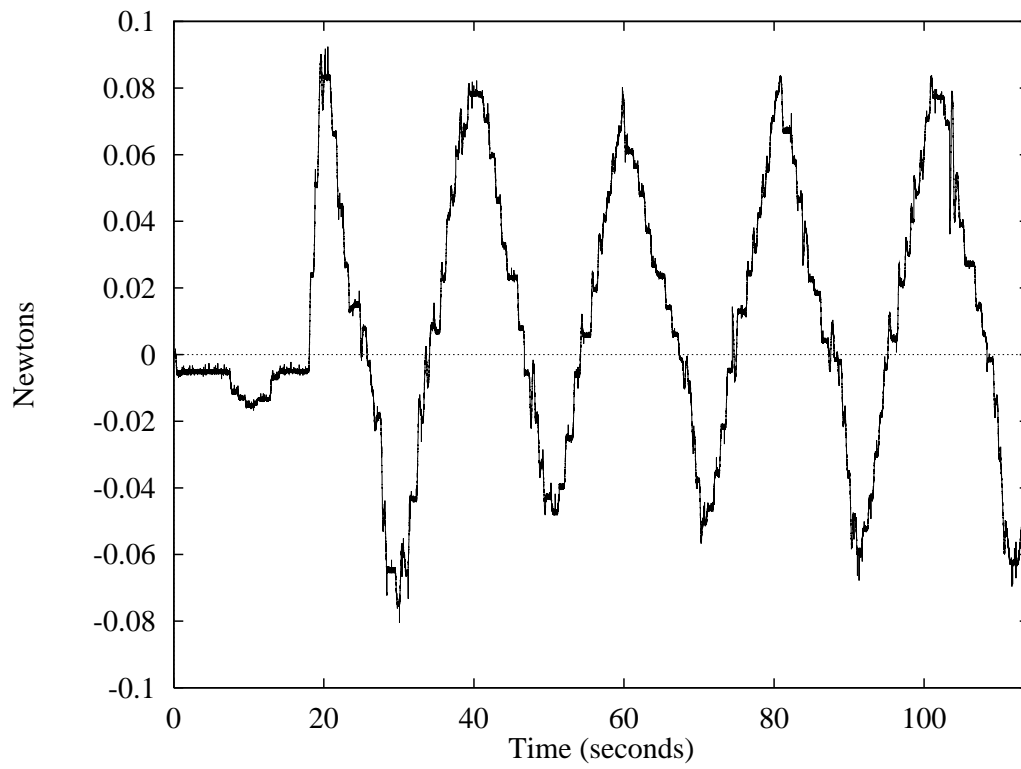


Figure 8:

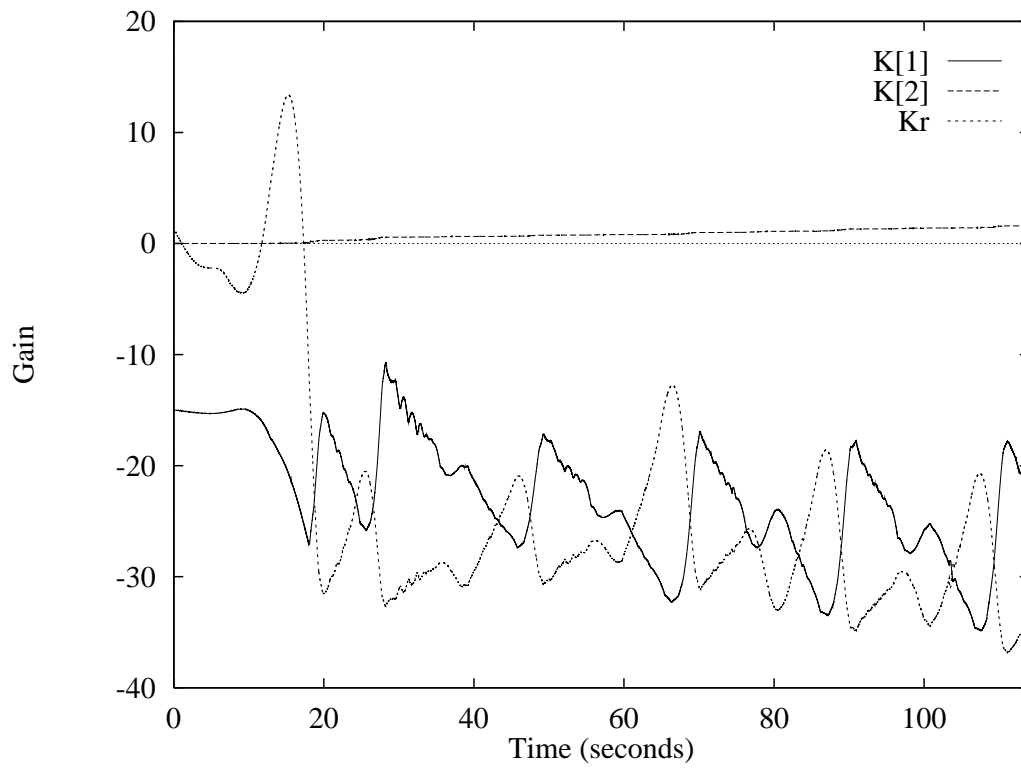


Figure 9: